IOSR Journal Of Applied Physics (IOSR-JAP)
e-ISSN: 2278-4861.Volume 16, Issue 4 Ser. 2 (July. – August. 2024), PP 14-19
www.Iosrjournals.Org

Dielectric Studies of $Pr_xY_{1-X}FeO_3$ Magneto-Electric (ME) Materials prepared by Sol-Gel route

T. Devender Reddy[1], G. Padmasree[2], P. Yadagiri Reddy[1], Ch. Gopal Reddy[1*]
[1]*Department Of Physics, Osmania University, Hyderabad – 500007, Telangana, India*
[2]*Stanley College Of Engineering & Technology For Women, Hyderabad- 500001, Telangana, India*

Abstract
$Pr_xY_{1-x}FeO_3$ (x = 0.0, 0.2, 0.4, 0.6, 0.8 and 1.0) magneto-electric samples are synthesized by sol-gel auto combustion method. Investigations on structural and dielectric studies of Praseodymium (Pr) substituted Yttrium ferrite ($YFeO_3$) samples are presented in this paper. Structural characterization of the samples is done by X-ray diffraction (XRD) and Field Emission Scanning Electron Microscope (FESEM) methods. XRD graphs show that the samples are crystalline in nature having single phase. From XRD measurements, unit cell parameters and cell volume are calculated. FESEM analysis indicates that all the samples have non-uniform grain size with increasing porosity with the content of Pr. Dielectric constant for all the samples is found to decrease with increasing frequency and increase with increasing temperature. Further, with the doping of Pr in $YFeO_3$, the dielectric constant at a given frequency exhibits increasing trend with the doping content except for x=1.0.

Keywords: *Sol-gel method, X-ray diffraction, FESEM, Dielectric constant.*

Date of Submission: 11-08-2024 Date of Acceptance: 21-08-2024

I. Introduction

Multiferroic materials have attracted great attention because of their diverse and important properties, including ferroelectricity, ferromagnetism and ferroelasticity [1]. Multiferroic materials exhibit many ferroic orders simultaneously, including ferromagnetism and ferroelectricity, making them attractive class of materials [2-4]. These multiferroics have an interesting feature called magneto-electric (ME) coupling, which combines magnetic and electric order [5, 6]. Multiferroics are widely used in wide range of applications, including storage devices, solar energy devices, transducers, sensors, bubble memory devices, permanent magnets, optoelectronics, satellite communication, etc. [7–9].

Because of diverse physical properties and uses in the present era of technology, orthoferrites having general formula $RFeO_3$ (where R is rare earth element) are gaining attention of scientific community [10–13]. At ambient temperatures, $RFeO_3$ polycrystalline materials have a distorted perovskite structure characterized by space group of P*nma* or P*bnm* [14]. Perovskite type orthoferrites exhibit unique structural, electrical and dielectric properties. Orthoferrites are synthesized by different methods such as solid-state reaction [15], combustion method [16], hydrothermal method [17], electron spin route [18] and co-precipitation method [19]. D. Triyono et al. [20] reported the synthesis of $La_{1-x}Sr_xFeO_3$ (x = 0.1, 0.2, 0.3, 0.4) by citrate auto-combustion method and studied the structural and dielectric properties. They used impedance spectroscopic technique to explain the electrical properties in relation to the frequency range (100 Hz to 1 MHz) under different temperatures. They found the existence of tiny polarons as charge carriers within the grain and grain border by electrical conductivity studies. Substitution of Sr at La site enhanced both the dielectric constant and electronic conductivity. M. Asif et al. [21] conducted a study on dielectric behavior of $Y_{1-x}Pr_xFeO_3$ ($0 \leq x \leq 0.16$) samples at ambient temperature. The study employed a wide frequency range from 1 MHz to 3 GHz. They observed that adding Pr considerably increased the dielectric constant.

Due to its magneto-optical phenomena, $YFeO_3$ perovskite can be used as memory element in logical devices, optical switches, magnetic field sensors and magnetic and optical current sensors [22]. $YFeO_3$ possesses perovskite structure with P*bnm* space group. The Y cation is coordinated by 12 oxygen anions, while the Fe cations are surrounded by six oxygen anions [23]. $YFeO_3$ exhibits weak ferromagnetism with Neel temperature T_N = 645 K and possesses a G-type antiferromagnetic nature. While two adjoining octahedral sites share oxygen, each ferric cation at the octahedral site in $YFeO_3$ is surrounded by six surrounding magnetic ions and organized as FeO_6. The Wagner space charge effect causes $YFeO_3$ to show ferroelectric behavior as well as a dielectric polarization mechanism. The activation of charge carriers between Fe^{2+} and Fe^{3+} ions is the cause of the dielectric relaxation phenomenon. Researchers are becoming more interested in it because, when compared to other multiferroics, $YFeO_3$ exhibits multiferroic features at ambient temperature.

The primary aim of present work is to analyze the effect of Praseodymium (Pr) doping on the structural, morphological and dielectric properties of the samples and an attempt is made to correlate them to the crystallographic changes occurring in the samples with Pr doping. Present work primarily focuses on investigating the changes occurring in the structural, morphological, and dielectric properties of $Pr_xY_{1-x}FeO_3$ samples.

II. Materials And Methods

Polycrystalline multiferroic $Pr_xY_{1-x}FeO_3$ (x=0.0, 0.2, 0.4, 0.6, 0.8 and 1.0) samples are prepared using sol-gel auto-combustion method. Yttrium oxide (Y_2O_3) is weighed in a stoichiometric ratio and dissolved in nitric acid (HNO_3) to form nitrates. Iron (III) nitrate nonahydrate [$Fe(NO_3)_3.9H_2O$] is dissolved in water and its clear solution is obtained. Citric acid is taken in 1:1 ratio with metallic ion and is dissolved in water. Praseodymium oxide (Pr_6O_{11}) is dissolved in nitric acid and is constantly stirred to obtain a clear solution. All the prepared solutions of Y_2O_3, $Fe(NO_3)_3.9H_2O$, citric acid and Pr_6O_{11} are added together and continuously stirred for 30 minutes. The p^H of the solution is adjusted to neutral by adding ammonium hydroxide (NH_4OH) solution drop wise and the neutral solution is heated and stirred continuously for 4 hours. When the volume of the solution is reduced to one-third of its original volume, ethylene glycol is added in a ratio of 1:1.2 to turn the solution into gel. The obtained gel is then heated at 150 °C until it turns into a brown fluffy ash. This ash is then finely grinded to get powder and is calcinated at 600 °C for 4 hours to remove volatile gases. These samples are then densely pelletized using pelletizer machine and sintered at 1200 °C for 4 hours in a hot furnace.

The Bruker D8 Advance X-Ray Diffractometer with Cu-K_α radiation is used for the XRD measurements, which are used to study the structural characteristics of the materials. The micrographs of the samples are recorded using a Field Emission Scanning Electron Microscope (FESEM) device (Carlzeiss Ultra 55 Model of Oxford), which provides information about the grain size and surface morphology of the samples. Dielectric measurements are carried out at room temperature and low temperature using a precision LCR meter E4980 coupled with an in-house developed sample holder, in the frequency range 0.5 kHz to 100 kHz.

III. Results And Discussion

Structural Analysis

Fig. 1 indicates Rietveld refined X-ray diffraction (XRD) graphs of praseodymium (Pr) doped yttrium iron oxide ($YFeO_3$) samples. The sharp peaks of the samples with high intensity indicate good crystallization. All these samples have distorted orthorhombic structure having space group P*bnm* [24-26]. Extra peaks are not observed in the XRD graphs which confirm that the samples are in pure phase form without any detectable impurity. The Rietveld refined parameter representing the goodness of fit (χ^2) for all the samples is found to be less than or around 2.0 indicating that the data fitting is good. Fig. 2 shows variation of lattice parameters (a, b, c) and unit cell volume (V) with change in concentration of praseodymium (Pr) doping. It is observed that lattice parameters and unit cell volume increase with the increase in praseodymium (Pr) concentration. When large sized praseodymium ion (Pr^{3+}) having ionic radius = 1.18 A^0 is substituted at the site of yttrium ion Y^{3+} with ionic radius = 0.90 A^0, it results in the change of crystal structure. The rotation around the orthorhombic crystallographic axis results in tilted FeO_6 octahedral structure. With increase in Pr concentration, the magnitude of tilting of FeO_6 octahedral structure also increases leading to increase of lattice parameters [27, 28]. The increase in lattice parameters indicates that doping of praseodymium in place of yttrium induces distortion in the crystal structure. These changes in unit cell parameters cause corresponding changes in Fe-O bond length and O-Fe-O bond angles that have prominent effects on electrical properties of these materials.

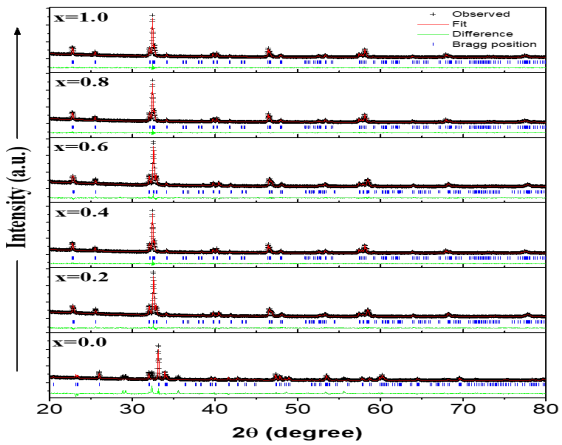

Fig. 1 Rietveld refined XRD graphs of $Pr_xY_{1-x}FeO_3$ samples

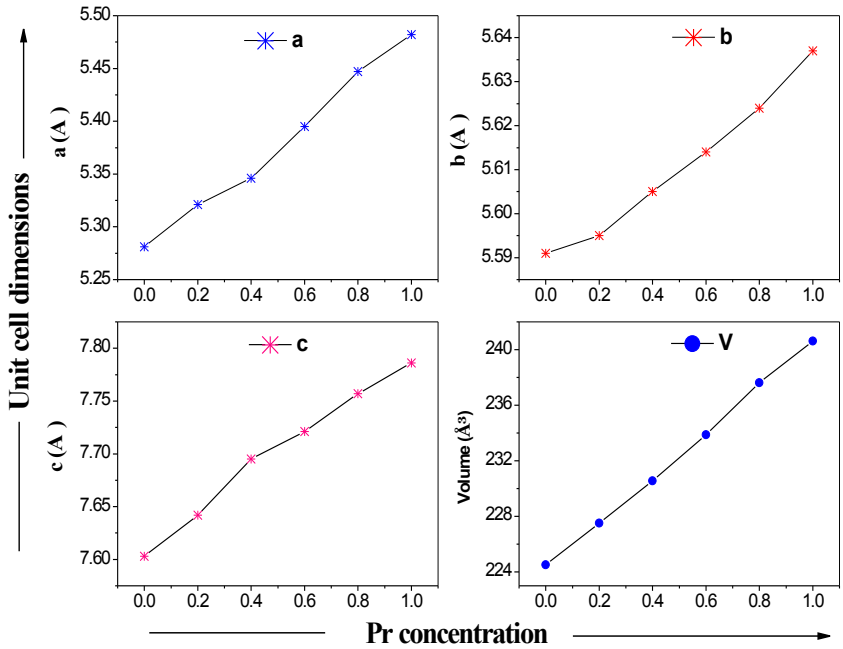

Fig. 2 Variation of lattice parameters (a,b,c) and unit cell volume (V) with Pr concentration (x)

Surface Morphological Analysis

To understand the micro-structure and arrangement of grains in the samples, Field Emission Scanning Electron Microscope (FESEM) images are obtained. Fig. 3 shows FESEM images of $Pr_xY_{1-x}FeO_3$ (x = 0.0, 0.2, 0.4, 0.6, 0.8 and 1.0) samples in the scale of 200 nm. All the samples have non-uniform grain size and the grains are irregular in shape and size. As the doping of the Pr increases, the grains are coalescing with each other and as a result the grain size decreases and porosity increases. This agglomeration of the grains results in the contact between the non-uniform grains leading to charge exchange between the grains called as hetero-charging [29]. The change in the grain structure and porosity induces modifications in the electrical properties of the samples.

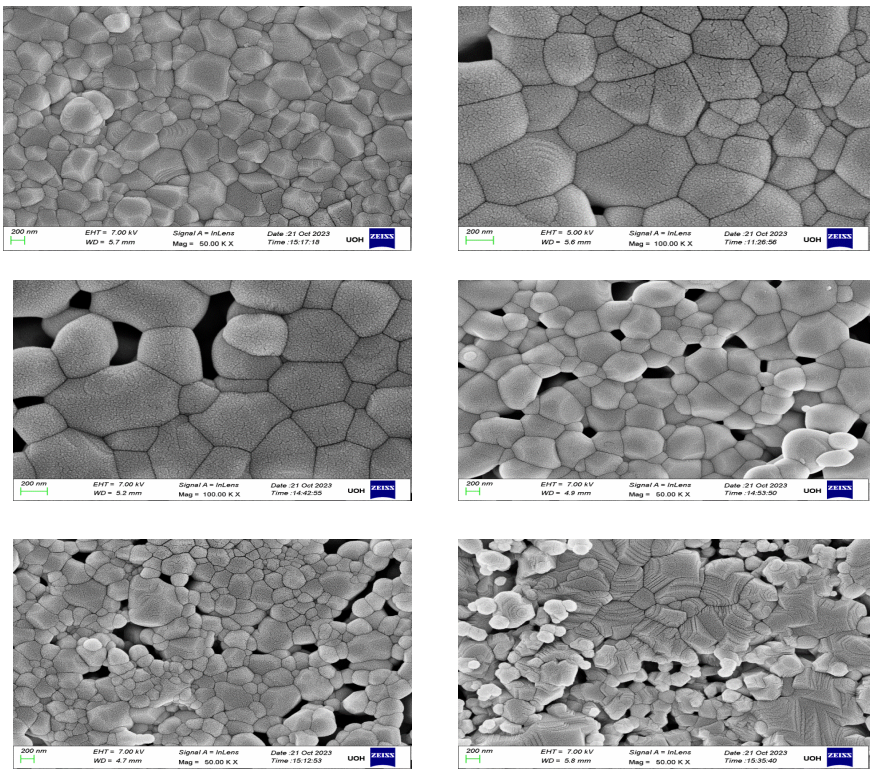

Fig. 3 FESEM images of $Pr_xY_{1-x}FeO_3$ samples

Dielectric constant measurements

Fig. 4 shows the variation of dielectric constant with frequency for the $Pr_xY_{1-x}FeO_3$ (x=0.0, 0.2, 0.4, 0.6, 0.8 and1.0) samples in the range of 0 Hz to 1 MHz. It is observed that the dielectric constant for all the samples tends to decrease as the frequency increases. The dielectric constant (ε) of prepared samples is given by the equation $\varepsilon = C.d/ (A.\varepsilon_o)$ [30], where C is the capacitance, d is the thickness of the pellet, A is the area of the pellet and ε_o is the permittivity of free space. It has been reported that the dielectric constant of metal oxides depends on various types of polarizations viz. interfacial or space charge polarization, ionic polarization, dipolar polarization and electronic polarization [31]. In the low frequency region, space charge or interfacial polarization dominates due to the accumulation of charges at grain boundaries. This is based on Koop's phenomenological theory. In the high-frequency region ionic and electronic polarization plays a vital role for polarization [32]. All samples show a normal dispersion behavior i.e. high value of dielectric constant at low frequency. At low-frequency dipoles have sufficient time for the alignment in the direction of the applied field, hence high value of the dielectric constant is observed. But at higher frequencies, dipoles could not synchronize with the applied field, as a result of which low value of the dielectric constant is observed for the samples.

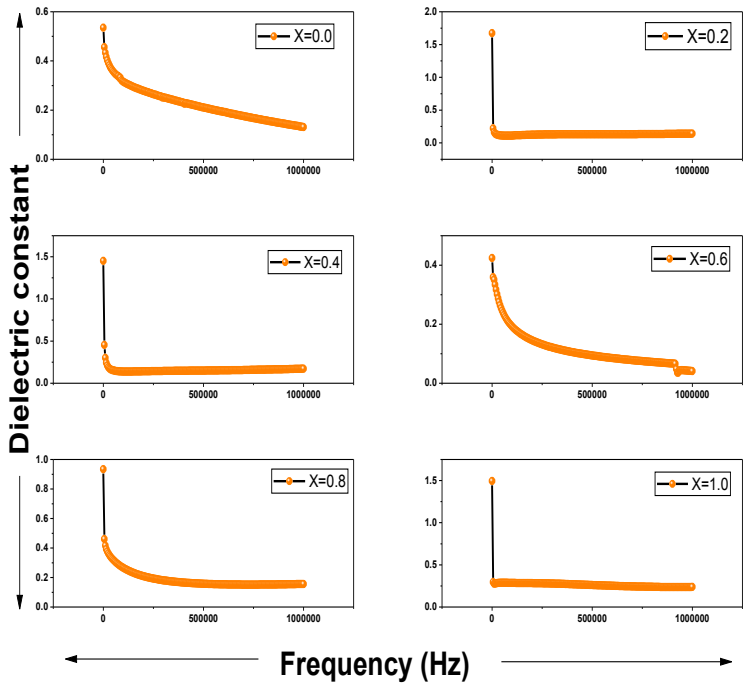

Fig. 4 Dielectric constant versus frequency response of $Pr_xY_{1-x}FeO_3$ samples at room temperature

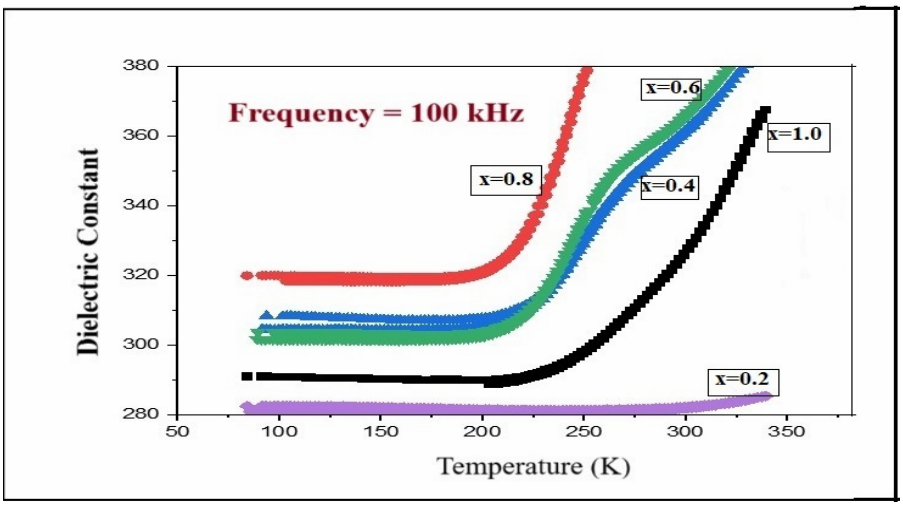

Fig. 5 Dielectric constant versus temperature response of $Pr_xY_{1-x}FeO_3$ samples at 100 kHz

Fig. 5 shows temperature-dependent variation of dielectric constant at 100 kHz frequency for all samples in the range of 80 K to higher temperatures. It is seen that the dielectric constant for each of the samples is almost constant at low temperatures up to about 200K. The reason for this may be that the thermal energy at low temperatures is insufficient to cause the relative movement of dipoles resulting in almost constant dielectric behavior. With further increasing temperature, there is a corresponding increase in the dielectric constant, which is in line with expected nature of orthoferrite materials [33]. Due to increase of temperature, the electric dipoles attain high thermal energy and orient in the direction of applied electric field, leading to an increase in electric polarization which increases the dielectric constant. It is also observed that the dielectric constants for the Pr doped $YFeO_3$ ($Pr_xY_{1-x}FeO_3$) samples at temperatures below 200K are approximately in the range of 280 to 320 with the dielectric constant increasing with increasing value of 'x' except for x = 1.0, for which it shows decreasing trend. The doping of Pr at Y site causes a change in relative positions of cations and anions which in turn changes structural parameters, such as bond lengths. The variation in bond lengths of Fe–O and Y–O influences the ionic interactions between cations and anions, thereby changing the dielectric constant. Further, it is seen from the FESEM images that as Pr concentration is increased, there is a change in the grain structure with increasing porosity which also affects the dielectrical properties of the samples.

IV. Conclusions

The multiferroic $Pr_xY_{1-x}FeO_3$ (x=0.0, 0.2, 0.4, 0.6, 0.8 and 1.0) samples are synthesized using sol-gel auto-combustion method. Rietveld refined XRD structural analysis shows that the samples are crystalline in nature and confirms that the samples possess distorted orthorhombic structure with space group P*bnm*. FESEM analysis shows non-uniform nature of grain size with increasing porosity. Dielectric constant decreases for all the samples with increase in frequency at room temperature and it increases with increasing temperature. It is further observed that the dielectric constant shows increasing trend with the Pr concentration in $Pr_xY_{1-x}FeO_3$ samples, except when the Yttrium is completely replaced by Pr, i.e. when x = 1.0. This may be attributed to changes in structural parameters, such as bond lengths, grain structure and porosity.

Acknowledgements

Authors thank UGC-DAE CSR, Indore, India for sanctioning a project under Collaborative Research Scheme (CRS) with Ref. No: CRS/2021- 22/01/376 for one of the authors (Dr. G. Padmasree) and providing the facilities to carry out the measurements. The authors thank Dr. Vasanth G. Sathe, Centre Director and Dr. V. Rghavendra Reddy, Scientist – H for giving an opportunity to work with UGC-DAE CSR, Indore. Special thanks to Mr. Anil Gome of UGC-DAE CSR, Indore for his support in obtaining XRD, electrical and dielectric measurements. We acknowledge FESEM-EDX facility at Department of Physics, University of Hyderabad for FESEM and EDX measurements.

References

[1] O. Rosales-González , F. Sánchez-De Jesús, C.A. Cortés-Escobedo, A.M. Bolarín-Miró, Crystal structure and multiferroic behavior of perovskite $YFeO_3$, Ceramics International, 44 (2018) 15298-15303.
[2] Bipul Deka, S. Ravi, A. Perumal, D. Pamu, Effect of Mn doping on magnetic and dielectric properties of $YFeO_3$, Ceramics International, 43 (2017) 1323-1334.
[3] Claude Ederer, Nicola A. Spaldin, Recent progress in first-principles studies of magnetoelectric multiferroics, Current Opinion in Solid State and Materials Science, 9 (2005) 128-139.
[4] L.W. Martin, R. Ramesh, Multiferroic and magnetoelectric heterostructures, Acta Materialia, 60 (2012) 2449-2470.
[5] Sukhendu Sadhukhan, Abhik S. Mahapatra, Ayan Mitra, Pabitra K. Chakrabarti, Multiferroic properties and magnetoelectric coupling observed in nanocrystalline HoFeO3, Journal of Alloys and Compounds, 907 (2022) 164443.
[6] G.E. Tongue Magne, R.M. KeumoTsiaze, A.J. Fotué, N.M. Hounkonnou, L.C. Fai, Cumulative effects of fluctuations and magnetoelectric coupling in two-dimensional RMnO3 (R = Tb, Lu and Y) multiferroics, Physics Letters A, 400 (2021) 127305.
[7] P. Iyyappa Rajan, S. Mahalakshmi, Sharat Chandra, Establishment of half-metallicity, ferrimagnetic ordering and double exchange interactions in Ni-doped BiFeO3 – A first-principles study, Computational Materials Science, 130(2017) 84-90.
[8] Subhash Sharma, Manish Kumar, Amel Laref, J.M. Siqueiros, O. Raymond Herrera, Recent advances in interfacial engineering and band-gap tuning of perovskite multiferroic heterostructures for high performance photovoltaic applications, Materials Letters, 331 (2023) 133490.
[9] Jiagang Wu, Zhen Fan, Dingquan Xiao, Jianguo Zhu, John Wang, Multiferroic bismuth ferrite-based materials for multifunctional applications: Ceramic bulks, thin films and nanostructures, Progress in Materials Science, 84 (2016) 335-402.
[10] C.L. Li, S.S. Zheng, G.O. Barasa, Y.F. Zhao, L. Wang, C.L. Wang, Y. Lu, Y. Qiu, J.B. Cheng, Y.S. Luo, A comparative study on magnetic behaviors and magnetocaloric effect in heavy rare-earth antiferromagnetic orthoferrites RFeO3 (R = Dy, Ho and Er), Ceramics International, 47 (2021) 35160-35169.
[11] M. Kamal Warshi, Vikash Mishra, Archna Sagdeo, Vinayak Mishra, Rajesh Kumar, P.R. Sagdeo, Structural, optical and electronic properties of RFeO3, Ceramics International, 44 (2018) 8344-8349.
[12] Zhao-Qi Wang, Yang-Shun Lan, Zhao-Yi Zeng, Xiang-Rong Chen, Qi-Feng Chen, Magnetic structures and optical properties of rare-earth orthoferrites RFeO3 (R = Ho, Er, Tm and Lu), Solid State Communications, 288 (2019) 10-17.
[13] T. Shen, C. Hu, W.L. Yang, H.C. Liu, X.L. Wei, Theoretical investigation of magnetic, electronic and optical properties of orthorhombic YFeO3: A first-principle study, Materials Science in Semiconductor Processing, 34 (2015) 114-120.
[14] B. Deka, S. Ravi, A. Perumal, D. Pamu, Efect of Mn doping on magnetic and dielectric properties of YFeO3, Ceramics International, 43 (2017) 1323-1334.

[15] C. Xiangfeng, P. Siciliano, CH3SH-sensing characteristics of LaFeO3 thick-flm prepared by co-precipitation method, Sensors and Actuators, B: Chemistry, 94 (2003) 197–200.
[16] X.-P. Xiang, L.-H.Zhao, B.-T.Teng, J.-J.Lang, X. Hu, T. Li, Y.-A.Fang, M.-F.Luo, J.-J. Lin, Catalytic combustion of methane on La1-xCexFeO$_3$ oxides. Applied Surface Science, 276 (2013) 328–332.
[17] S. Thirumalairajan, K. Girija, I. Ganesh, D. Mangalaraj, C. Viswanathan, A. Balamurugan, N. Ponpandian, Controlled synthesis of perovskite LaFeO3 microsphere composed of nanoparticles via self-assembly process and their associated photocatalytic activity, Journal of Chemical Engineering, 209 (2012) 420–428.
[18] J. Leng, S. Li, Z. Wang, Y. Xue, D. Xu, Synthesis of ultrafne lanthanum ferrite (LaFeO3) fibers via electrospinning, Material Letters, 64 (2010) 1912–1914.
[19] G. Pecchi, P. Reyes, R. Zamora, C. Campos, L.E. Cadús, B.P. Barbero, Effect of the preparation method on the catalytic activity of La1-xCaxFeO3 perovskite-type oxides, Catalysis Today, 133–135 (2008) 420-427.
[20] D. Triyono, C.A. Kafa, H. Laysandr, Efect of Sr-substitution on the structural and dielectric properties of LaFeO3 perovskite materials, Journal of Advanced Dielectrics, 8 (2018) 1850036.
[21] M. Asif, M. Azhar Khan, S. Atiq, T. Alshahrani, Q. Mahmood, N.A. Kattan, A. Manzoor, Evolution of structure and improvement in dielectric properties of praseodymium substituted $YFeO_3$ nanomaterials synthesized via a sol-gel auto-combustion method, Ceramics International, 47 (2021) 6663–6674.
[22] Man Cheng, Guojian Jiang, Wenqian Yang, Li Duan, Wei Peng, Jiang Chen, Xiaojian Wang, Study of $Y_{1-x}Er_xFeO_3$ ($0\leq x\leq 1$) powder synthesized by sol–gel method and their magnetic properties, Journal of Magnetism and Magnetic Materials, 417 (2016) 87-91.
[23] T. Nishimura, S. Hosokawa, Y. Masuda, K. Wada, M. Inoue, Synthesis of metastable rare-earth–iron mixed oxide with the hexagonal crystal structure, Journal of Solid State Chemistry, 197 (2013) 402–407.
[24] R Saha , A Sundaresan, CNR Rao, Novel features of multiferroic and magnetoelectric ferrites and chromites exhibiting magnetically driven ferroelectricity, Materials Horizon, 01 (2014) 20–31.
[25] S Geller, EA Wood, Crystallographic studies of perovskite like compounds: I. Rare earth orthoferrites and $YFeO_3$, $YCrO_3$,$YAlO_3$, Acta Crystallography, 9 (1956) 563–568.
[26] H Shen , J Xu , G Jin Mand Jiang, Influence of manganese on the structure and magnetic properties of YFeO3 nanocrystal, Ceramics International, 38 (2012) 1473–1477.